LLMS Adaptive Array Beamforming Algorithm for Concentric Circular Arrays

Jalal Abdulsayed SRAR[1,2], Kah-Seng CHUNG[2] and Ali MANSOUR[2]

[1]Dept. of Electrical and Electronic Engineering, Misurata University, Misurata, Libya
[2]Dept. of Electrical and Computer Engineering, Curtin University of Technology,
Perth, Australia
jalal.srar@gmail.com, k.chung@curtin.edu.au, and mansour@ieee.org

Abstract. An improvement of Signal-to-Interference Ratio (SIR) at the base station of a wireless communication system can be obtained using a suitable choice of an array antenna. In this paper we consider Concentric Circular Antenna Array (CCAA) which can be used for adaptive antenna systems. A new adaptive algorithm, called least mean square-least mean Square (LLMS) algorithm, has been proposed for different applications of array beamforming. Unlike earlier LMS algorithm based techniques, the proposed algorithm derives its overall error signal by feeding back the error signal from the second LMS algorithm stage (LMS_2) to combine with that of the first LMS algorithm section (LMS_1). In this paper, we employ the LLMS beamforming algorithm for a CCAA system. The mathematical model of CCAA is analyzed. Computer simulation results show that employing LLMS algorithm is superior in convergence; and beam pattern performances over earlier LMS based algorithms. Furthermore, CCAA LLMS beamforming is more robust compared with other algorithms when operating in the presence of Rayleigh fading. Fidelity of the recovery signal of all algorithms under test is demonstrated by means of the resultant values of Error Vector Magnitude (EVM) and scatter plots.

Keywords: CCAA, Adaptive array beamforming, EVM, LLMS and LMS algorithms, Rayleigh fading.

1 Introduction

In recent years, adaptive or smart antennas have become a key component for various wireless applications, such as radar, sonar and cellular mobile communications [1] including worldwide interoperability for microwave access (WiMAX) [2] and recently in Long Term Evolution (LTE) [3]. They lead to an increase in coverage range and capacity for these systems and mobile system in particular. This is because these antennas are used as spatial filters for the desired signal coming from specific direction/s while minimizing the reception of unwanted signals emanating from other directions. Beamforming is central to all antenna arrays, and a summary of beamforming techniques is presented in [4].

There are many configurations of antenna arrays elements; they may linear, planar

or circular arrangement. Nowadays, circular arrays (CA) have become very popular over other array geometries because they have the ability for all-azimuth scan without a considerable change in the beam pattern. Moreover, since CA does not have edge elements, it has less effect by the mutual coupling as compared with Linear Array (LA) and rectangular array (RA) [5, 6]. CCAA configuration may contain many concentric circular rings with different number of elements and radii, which has more flexibility in the array pattern synthesis both in narrow and broad bands applications [6].

Many beamforming algorithms have been proposed in the literature, which include LMS based algorithms [5-10], to optimize the element weighting. Examples such as normalized-LMS (NLMS) [7], variable-length LMS algorithm [8], transform domain algorithms [8], and recently constrained-stability LMS (CSLMS) algorithm [10] and modified robust variable step size LMS (MRVSS) algorithm [11].

More recently, a different approach has been presented in [12], which consists of two LMS algorithms stages interconnected via an array image vector ( ). This algorithm is called the LLMS algorithm, which overcomes many of the drawbacks associated with previous use of combined algorithms.

With the proposed LLMS algorithm scheme, as shown in Fig. 1, the intermediate output, y_{LMS1}, yielded from the first LMS or LMS_1 algorithm section, is multiplied by the array image vector, **,** of the desired signal. The resultant "filtered" signal is further processed by the second LMS algorithm or LMS_2 algorithm section. For the adaptation process, the error signal of LMS_2 algorithm, e_2, is fed back to combine with that of LMS_1 algorithm, to form the overall error signal, e_{LLMS}, for updating the tap weights of LMS_1 algorithm. As shown in Fig. 1, a common external reference signal is used for both the two LMS algorithm sections, i.e., d_1 and d_2. Moreover, this external reference signal may be replaced by y_{LMS1} in place of d_2, and y_{LLMS} for d_1 to produce a self-referenced version of the LLMS algorithm scheme.

For the case of a moving target, it is necessary that the array image vector, **,** is made adaptive in order to follow the angle of arrival (AOA) of the wanted signal. A simple yet effective method of estimating is also presented in [12]. This adaptive version is simply known as LLMS algorithm in order to differentiate it from the scheme that makes use of prescribed**,** which referred to as $LLMS_1$ algorithm.

The mathematical analysis of the error convergence for the external referencing, self-referencing and the adaptive cases have been shown in [12]. The results published in [12] show that the LLMS algorithm, when used in a beamforming application, converges faster than either the LMS, CSLMS or MRVSS algorithms. Also, the convergence is less sensitive to variations in the input signal to noise ratio (SNR). Furthermore, the results showed that, the LLMS algorithm can operate with a noisy reference signal.
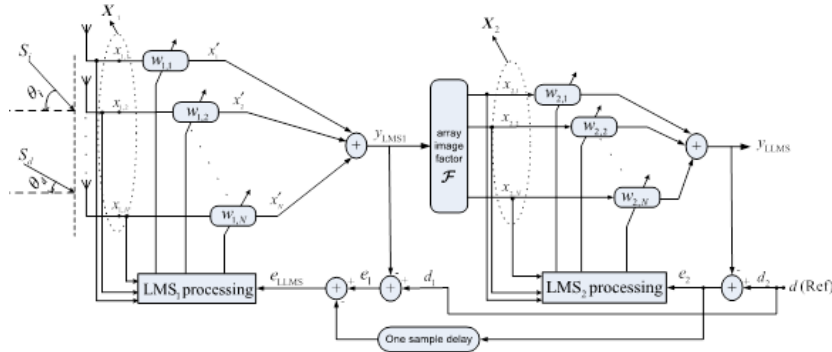
Fig.1. The LLMS algorithm with an external reference signal [12]

In this paper, we further study the central feeding CCAA beamforming that employs LLMS algorithm instead of LA scheme. The error convergence, EVM and beam pattern are examined for both modes of operation; LLMS1 and LLMS. Operation for fast changing signal environment is also examined to make sure that this algorithm is able to work under Raleigh fading channel. CSLMS and MRVSS algorithms have shown improved performance over other published algorithms; therefore they have been used in this paper for performance comparison with the LLMS algorithm.

After the description of the array steering vector of Uniform CCAA (UCCAA) in Section II, mathematical expressions of the signal model are derived in Section III. In Section IV, the design parameters of UCCAA are analyzed to find the relation between the rings radii and the number of elements. Computer environment and simulation results obtained for 3 rings of 2, 4 and 6 element array are presented in Sections V and VI respectively. Finally, in Section VII, we conclude the paper.

2 Array Steering Vector of CCAA

CCAA element arrangement may contain multiple concentric rings with different elements and radii such that shown in Fig. 2. As a result, the radiation pattern will differ from that of LA.

Let us consider a CCAA with M concentric circular rings with radius r and a number of omnidirectional antenna elements in each ring as N_m, as shown in Fig. 2, where $m = 1, 2, \ldots, M$.

Now, to simplify the expressions, let us define the array steering vector for a single ring, then we extend the analysis for the whole array. For the mth ring, the complex array vector for the desired ($\square_{d,m}$) and the cochannel interfered ($\square_{i,m}$) signals can be written as

$$\square_{d,m}(\theta, \phi) = [e^{j\psi_{d,m} \cos(\phi - \phi_{m1})} \; e^{j\psi_{d,m} \cos(\phi - \phi_{m2})} \; \ldots$$
$$e^{j\psi_{d,m} \cos(\phi - \phi_{mN_m})}]^T \tag{1}$$

$$\square_{i,m}(\theta,\phi) = [e^{j\psi_{i,m}\,cos(\phi-\phi_{m1})} \; e^{j\psi_{i,m}\,cos(\phi-\phi_{m2})} \; ....$$

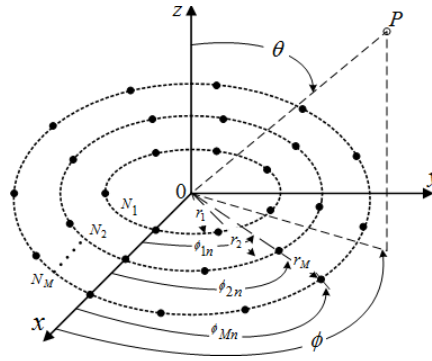$$e^{j\psi_{i,m}\,cos(\phi-\phi_{mN_m})}]^T \tag{2}$$

Fig. 2. Concentric circular arrays (CCAA)

According to the far-field plane wave model, $\psi_{d,m} = \frac{2\pi}{L} r_m sin(\theta_d)$, $\psi_{i,m} = \frac{2\pi}{\lambda} r_m sin(\theta_i)$ and $(g)^T$ denotes the Transpose matrix of (g).

Now, for the whole array, we combine the array vectors for all rings in one matrix to form the total steering matrices for the desired and interfered signals, such as

$$\square_{Td}(\theta,\phi) = [\square_{d,1}(\theta,\phi) \, \square_{d,2}(\theta,\phi) \, ... \square_{d,m}(\theta,\phi)$$
$$... \square_{d,M}(\theta,\phi)] \tag{3}$$

$$\square_{Ti}(\theta,\phi) = [\square_{i,1}(\theta,\phi) \, \square_{i,2}(\theta,\phi) \, ... \square_{i,m}(\theta,\phi)$$
$$... \square_{i,M}(\theta,\phi)] \tag{4}$$

Since the rings may have different number of elements, the array vectors have unequal lengths. Mathematically, to overcome this problem, we add zeros to the lower dimension vectors. Actually, the outer rings will have more antenna elements than the next inner one. Therefore, the outermost ring will have N_m elements; consequently, the size of the steering matrix will be $N_m \times M$. For example, the steering matrix for the desired signal could be written as:

$$\square_{Td}(\theta,\phi) =$$

$$\begin{bmatrix} e^{j\psi_{d,1}\,cos(\phi-\phi_{11})} & e^{j\psi_{d,2}\,cos(\phi-\phi_{21})} & ... & e^{j\psi_{d,M}\,cos(\phi-\phi_{M1})} \\ e^{j\psi_{d,1}\,cos(\phi-\phi_{12})} & e^{j\psi_{d,2}\,cos(\phi-\phi_{22})} & ... & e^{j\psi_{d,M}\,cos(\phi-\phi_{M2})} \\ . & . & . & . \\ e^{j\psi_{d,1}\,cos(\phi-\phi_{1N_1})} & . & . & . \\ 0 & e^{j\psi_{d,2}\,cos(\phi-\phi_{2N_2})} & . & . \\ 0 & 0 & . & . \\ 0 & 0 & ... & e^{j\psi_{d,M}\,cos(\phi-\phi_{MN_{M-1}})} \\ 0 & 0 & ... & e^{j\psi_{d,M}\,cos(\phi-\phi_{MN_M})} \end{bmatrix}$$

$$(5)$$

The case is similar for the interfered signal; $\square_{Ti}(\theta, \phi)$.

I. SIGNAL MODEL

Let $s_d(t)$ and $s_i(t)$ be the desired and interfering signals, respectively. Then, the input signals of the array, in the time domain, can be expressed as

$$x_1(t) = \square_{Td}\, s_d(t) + \square_{Ti}\, s_i(t) + n(t) \qquad (6)$$

where $n(t)$ is the additive white Gaussian noise matrix with size as $N_m \times M$.

With respect to Fig. 2, the output of the LLMS beamformer can be expressed as [13],

$$y_{LLMS}(t) = SUM\{w_{\text{LLMS}}^H(\theta, \phi)x_1(\theta, \phi)\} \qquad (7)$$

where $w_{\text{LLMS}}^H = w_2^H \square_{\text{T}} w_1^H$ with w_1 and w_2 being the weight matrices for the first and second LMS algorithms stages, respectively. $(g)^H$ denotes the Hermitian transpose of (g).

II. UNIFORM CONCENTRIC CIRCLE ANTENNA ARRAY UCCAA

In UCCAA scheme, the number of elements in each ring (N_m), the element-arc-separation (c_m) and the ring-radial-separation (d_m) will affect the array performance such as error convergence and beam pattern. Therefore, the analysis and relation between N_m, c_m, and d_m will be considered in this section.

Assuming the normalized elements-arc-separation (c_m) in each ring are uniformly separated [13], *i.e.*,

$$c_m = \frac{2\pi r_m}{N_m \lambda} \qquad (8)$$

From (8), the normalized ring radius ($\hat{r}_m$) can be calculated from

$$\hat{r}_m = \frac{c_m N_m}{2\pi} \qquad (9)$$

From (9), the ring-radial-separation (d_m) between any two successive rings will be

$$d_m = \hat{r}_{m+1} - \hat{r}_m \qquad (10)$$

Assume that the element-arc-separation (c_m) is fixed and equals to $\lambda/2$. Then from (8), the element increment (ΔN) between any two successive rings can be found as

$$\Delta N = 4\pi d_m \qquad (11)$$

Therefore, the total number of elements in the whole CCAA will

$$N_t = MN_1 + \sum_{k=1}^{M-1} k\Delta N \qquad (12)$$

3 Simulation Environment

The performance of the proposed LLMS algorithm in CCAA beamforming has been evaluated by means of simulations. For comparison purposes, results obtained with the conventional LMS, CSLMS and MRVSS algorithms are also presented. For the simulations, the following parameters are used:

- An isotropic UCCAA of 3 rings, with number of elements in the inner ring; $N_1 = 2$, middle ring; $N_2 = 4$ and the external ring $N_3 = 6$.
- Elements-arc-separation (c_m) is 0.5λ.
- To fix ΔN as 2 elements, the ring-radial-separation is chosen to be $0.5\lambda/\pi$.
- $r_1 = 0.5\lambda$, $r_2 = 0.66\lambda$ and $r_3 = 0.82\lambda$.
- A desired binary phase shift keying (BPSK) arrives at an angle of $(\theta, \phi) = (90, 30)$.
- An AWGN channel.
- All weight vectors are initially set to zero.
- A BPSK interference signal arrives at $(\theta, \phi) = (90, -30)$ with the same amplitude as the desired signal.

To facilitate comparison with the published algorithms; such as CSLMS algorithm in [10] and MRVSS algorithm in [11], a brief outline of the weight adaptation process of these algorithms is given here.

According to [10], the weights of the CSLMS algorithm are adapted as follow:

$$w(j + 1) = w(j) + \frac{\mu(j)}{\|\delta w(j)\|^2 + \epsilon} \delta x(j) \left(\delta e^{[j]}(j) \right)^*, \quad (13)$$

where ϵ is a small constant and is adjusted to yield the best possible performance in the operating-environment under consideration , and

$$\delta w(j) = w(j) - w(j - 1),$$
$$\delta x(j) = x(j) - x(j - 1),$$
$$\delta e^{[j]}(j) = e^{[j]}(j) - e^{[j]}(j - 1),$$
$$\text{and} \quad e^{[k]}(j) = d(j) - w^H(k)x(j),$$

As for the MRVSS algorithm [11], the step size, $\mu(j)$, is updated, such that

$$\mu(j + 1) = \begin{cases} \mu_{max} \ ; & \text{if } \mu(j + 1) > \mu_{max} \\ \mu_{min} \ ; & \text{if } \mu(j + 1) < \mu_{min} \\ \alpha\mu(j) + \gamma P^2(j) & \text{Else} \end{cases},$$

with $P(j + 1) = \left(1 - \beta(j)\right)P(j) + \beta(j)e(j)e(j - 1)$,

and $\beta(j + 1) = \begin{cases} \beta_{max} \ ; & \text{if } \beta(j + 1) > \beta_{max} \\ \beta_{min} \ ; & \text{if } \beta(j + 1) < \beta_{min} \\ \eta\beta(j) + \upsilon P^2(j) & \text{Else} \end{cases}$,

where $\alpha > 0, \eta > 1, (\gamma, \upsilon) > 1$,and $P(j)$is the time averaged error correlation over two consecutive values. The time averaged error square signal is β with its upper and lower bounds as β_{max} and β_{min}, respectively. The upper and lower bounds of μ, are μ_{max} and μ_{min}, respectively.

Table I tabulates the values of the various constants adopted for the simulations of the five different adaptive algorithms. The parameter values for the MRVSS algorithm operating in an AWGN channel are those given in [11]. All other values adopted here for the MRVSS and CSLMS algorithms have been chosen for obtaining the best performance out of these algorithms.

Often, performance comparison between different adaptive beamforming schemes is made in terms of the convergence errors and resultant beam patterns. Moreover, for a digitally modulated signal, it is also convenient to make use of the error vector magnitude (EVM) as an accurate measure of any distortion introduced by the adaptive scheme on the received signal at a given SNR. EVM is defined as [12]

$$EVM_{\text{RMS}} = \sqrt{\frac{1}{KP_o}\sum_{j=1}^{K}|S_r(j) - S_t(j)|^2} , \qquad (14)$$

where K is the number of used symbols, $S_r(j)$ is the jth output of the beamformer, and $S_t(j)$ is the jth transmitted symbol. P_o is the average power of all symbols for the given modulation.

Table 1. Values Of The Constants Used In Simulation

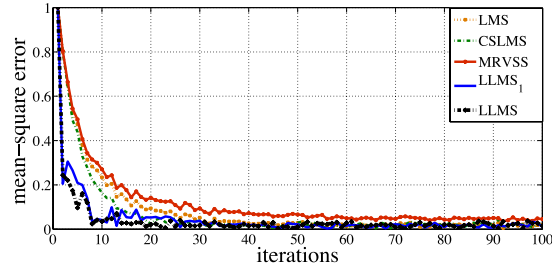| Algorithm	AWGN Channel	Rayleigh Fading Channel
LMS	$\mu = 0.02$	$\mu = 0.01$
LLMS$_1$	$\mu_1 = 0.02, \mu_2 = 0.03$	$\mu_1 = \mu_2 = 0.025$
LLMS	$\mu_1 = \mu_2 = 0.02$	$\mu_1 = 0.025, \mu_2 = 0.03$
CSLMS	$\mu = 0.01, \epsilon = 1$	$\mu = 0.01, \epsilon = 1.5$
MRVSS	$\beta_{max} = 0.017, \beta_{min} = 0,$ $\nu = 5 \times 10^{-4}, \mu_{max}$ $= 0.1, \mu_{min} = 1 \times 10^{-3}$ Intial $\mu = \mu_{max}, \alpha = 0.97$ $\gamma = 4.8 \times 10^{-4}, \eta = 0.97$	$\beta_{max} = 0.17, \beta_{min} = 0,$ $\nu = 5 \times 10^{-4}, \mu_{max}$ $= 0.02, \mu_{min} = 1 \times 10^{-4}$ Intial $\mu = \mu_{max}, \alpha = 0.97$ $\gamma = 4.8 \times 10^{-4}, \eta = 0.97$

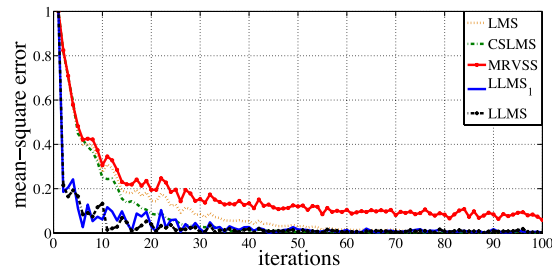## 4 Simulation Results

A. MSE Performance

First, the performances of the LLMS, LLMS$_1$, CSLMS, MRVSS and LMS algorithm schemes have been evaluated for UCCAA beamforming for three different cases of elevation angles. Those cases are the worse case; i.e at angles of $\theta_d = 0º$ and $\theta_i = 0º$, $\theta_d = 45º$ and $\theta_i = 45º$ and $\theta_d = 90º$ and $\theta_i = 90º$. The results for different SNR values have been studied in [12] in the case of LA, therefore, in this paper, the results are obtained only at $SNR = 10\ dB$. The convergence performances of these schemes are compared based on the ensemble average squared error $(\tilde{e}^2)$ obtained from 100 Monte Carlo simulation runs. Fig. 3a shows the worst case where the desired and interfered signals arrive from the same elevation angle; i.e, $\theta_d = \theta_i = 0º$. Figs. 3b and 3c show less stressed conditions. It is observed that under the given conditions, the two variants of the proposed LLMS algorithm converge faster than the other three scheme. Furthermore, their error floors are less sensitive to variations in the elevation angles, even for θ_d and θ_i as small as $0º$.

As for the CSLMS and MRVSS algorithms, they share the same performance for all the three considered elevation angles of arrive. As expected, the conventional LMS
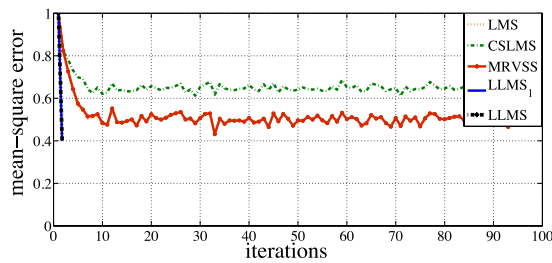
algorithm converges the slowest among the five algorithms. Also, simulations show that changing the azimuth angle while fixing the elevation angle will slightly change the convergence performance.

(c) $\theta_d = 90^o, \phi_d = 30^o, \theta_i = 90^o,$ and $\phi_i = -30^o$

(b) $\theta_d = 45^o, \phi_d = 30^o, \theta_i = 45^o,$ and $\phi_i = -30^o$

(a) $\theta_d = 0^o, \phi_d = 30^o, \theta_i = 0^o,$ and $\phi_i = -30^o$

Fig. 3. Two different convergence cases of LLMS, LLMS$_1$, CSLMS, MRVSS and LMS algorithms with the parameters given in the 2nd column of Table I, and SNR $= 10dB$.

Since, the elements of the array image vector ☐ of LLMS algorithm are being determined adaptively, this can influence its convergence behavior as it gives more smoothing error floor as shown in Fig. 3.

B. Beam Pattern Performance

In this experiment, two cases of cochannel interferences have been investigated in

the AWGN channel. Fig. 4a, shows the beam pattern for the five algorithms when single interfered signal arrives from $(\theta_i, \phi_i) = (90^o, -30^o)$ is used. In addition, Fig. 4b shows more investigations which are conducted for two interfered signals coming from $(\theta_{i1}, \phi_{i1}) = (90^o, -30^o)$ and $(\theta_{i2}, \phi_{i2}) = (90^o, -60^o)$.

In this study, a SNR of 10 dB is used. It is shown in Figs. 4a and 4b that the correct beam patterns can still be achieved using LLMS and LLMS$_1$ algorithms, however, the interference rejection for the two LLMS algorithm schemes is higher than the others as shown clearly in Table II. In fact, Table II shows the output (SIRo) for all the five algorithms when single interfered signal is used in one case, and double interfered signals in the other. From Table II, we can conclude, as expected, that the number of interfered signals increased, the SIRo decreased. However, both LLMS schemes have less affected by this increase.
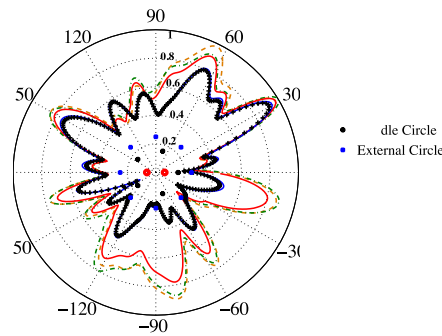
(a) The desired signal arrives $(\theta_d, \phi_d) = (90^o, 30^o)$ and one interfered signal arrives from $(\theta_i, \phi_i) = (90^o, -30^o)$
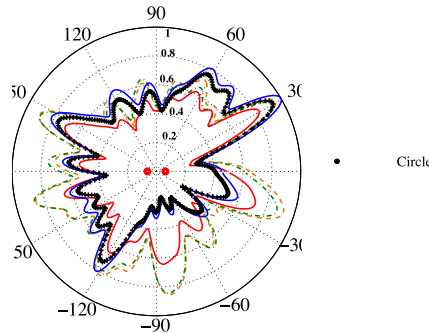
(b) The desired signal arrives $(\theta_d, \phi_d) = (90^o, 30^o)$ and two interfered signals arrive from $(\theta_{i1}, \phi_{i1}) = (90^o, -30^o)$ and $(\theta_{i2}, \phi_{i2}) = (90^o, -60^o)$

Fig. 4. The beam patterns achieved with the LLMS, LLMS$_1$, CSLMS, MRVSS and LMS algorithms with the parameters given in the 2nd column of Table I, and SNR $= 10dB$.

C. EVM and Scatter Plot

The performances of the five algorithms, based on the rms EVM computed using (14), for values of input SNR ranging from -5–25 dB in steps of 1 dB are shown in Fig. 5. These EVM values have been calculated after each of the adaptive algorithms has converged. It is observed that both the proposed LLMS and $LLMS_1$ algorithms achieve the lowest EVM values. Such superior performance becomes even more pronounced at lower values of input SNR. This further confirms the observation made from Fig. 2 in [12] showing that the operations of $LLMS_1$ and LLMS algorithms are very insensitive to changes in input SNR.

D. Operation in flat Rayleigh fading channel

The ability of an adaptive beamformer to operate in a dynamic environment is examined by subjecting the input signals to undergo flat Rayleigh fading. In this case, the rms EVM is again used as the performance metric for comparing the different adaptive beamforming algorithms. The following conditions are considered in the performance evaluation by computer simulations:

Table 2. SIR_o values obtained at SNR = 10 db

Algorithm	Output SIR (SIR_o) - *dB*	Output SIR (SIR_o) - *dB*
	One Interfered Signal	Two Interfered Signals
LMS	6.17	-0.62
CSLMS	6.7	-0.44
MRVSS	7.69	0.86
$LLMS_1$	13.04	6.14
LLMS	13.48	6.82

- The signals arriving at each antenna element, for both the desired and interference, undergo independent flat Rayleigh fading.
- The parameters as tabulated in column 3 of Table I are adopted for the different algorithms.
- Each simulation involves a run of 16 Mbits.
- Doppler frequency f_d = 120 Hz, corresponding to a mobility of 144 km/h at 900 MHz.
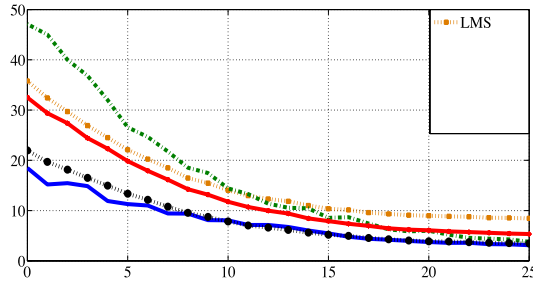
Fig. 5. The EVM values obtained with LLMS, LLMS$_1$, CSLMS, MRVSS and LMS algorithms at different input SNR with the parameters given in the 2nd column of Table I.

Fig. 6 shows the resultant EVM values as a function of the input SNR achieved for cochannel interference. From this figure, the following observations are made:

- All the five algorithms are able to operate in the presence of Rayleigh fading, however MRVSS shows more influence than other at higher SNR values.
- Both LLMS scheme algorithms are the least affected by Rayleigh fading.
- At SNR values less than zero, LMS algorithm is the most affected, while CSLMS is less, opposite to the case of no-fading as in Fig. 5. This is because the parameters used in a no-fading and a fading cases are different.
- Because of the differences in the parameter values that shown in the 2nd and 3rd columns of Table I, the results in Figs. 5 and 6 are slightly different, particularly for the results for SNR values higher than 10 dB.

Next, the scatter plots of the BPSK signal recovered using the adaptive beamformer, based on LMS, CSLMS, MRVSS, LLMS$_1$ and LLMS algorithms are shown in Figs. 7(a)–(e), respectively. The scatter plots are obtained from 100 signal samples for an input SNR $= 10$ dB and SIR $= 0$ dB. Again, the scatter plots of LLMS$_1$ and LLMS algorithms show the least spreading, indicating their ability to retain the signal fidelity.
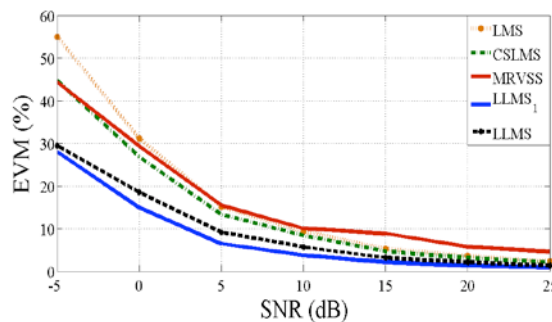

Fig. 6. The EVM values obtained with the LLMS, LLMS$_1$, CSLMS, MRVSS and LMS algorithms for different input SNR in the presence of Rayleigh fading with one interfered signal
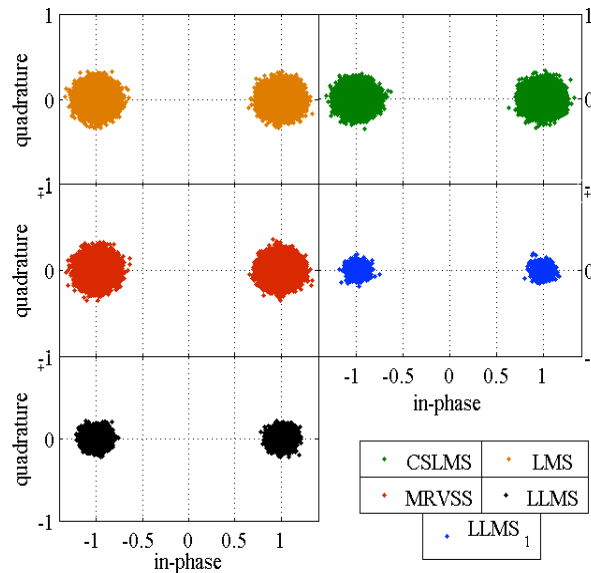
Fig. 7. The scatter plots of the recovered BPSK signal obtained with (a) LMS, (b) CSLMS, (c) MRVSS, (d) $LLMS_1$, and (e) LLMS algorithms for input $SNR = 10\,dB$ and $SIR = 0\,dB$.

5 Conclusions

This paper introduces our new algorithm, called LLMS algorithm, for CCAA beamforming. The mathematical model has been analyzed including array dimensions and number of elements per ring. The algorithm is simulated with external referencing mode.

It is shown that the LLMS algorithm performs quite similarly to the $LLMS_1$ algorithm. The two variants of the LLMS algorithm scheme are shown to have rapid convergence, typically within a few iterations. Also, unlike the MSE of the conventional LMS, CSLMS and MRVSS algorithms, the resulting steady state MSE of the $LLMS_1$ and LLMS algorithms is quite insensitive to the elevation angle. Moreover, the resultant EVM values and scatter plots obtained for operation in the presence of Rayleigh fading further demonstrate the superior performance of LLMS and $LLMS_1$ algorithms over the other three LMS-based algorithm schemes in a fast changing signal environment.

From the study of the interference influence on the desired signal, it is observed from the beam pattern that the LLMS algorithm schemes outperform the other three algorithms.

The superior performance of the proposed LLMS algorithm has been achieved with a complexity slightly larger than twice the conventional LMS algorithm scheme. Moreover, its complexity is lower than the MRVSS algorithm, and approximately the same as CSLMS algorithm.

References

1. N. A. Mohamed and J. G. Dunham, "Adaptive beamforming for DS-CDMA using conjugate gradient algorithm in a multipath fading channel," in Proc. IEEE Emerging Technologies Symposium on Wireless Communications and Systems, Richardson, USA, April 1999, pp. 1-5.
2. S. Chandran, "Performance of adaptive antenna arrays in the presence of varying noise power in WiMAX applications," in Proc. IET Int. Conf. on Wireless, Mobile and Multimedia Networks, Mumbai, India, Jan. 2008, pp. 3-5.
3. Massimiliano Ricci, Beam-Forming and Power Control in Flexible Spectrum Usage for LTE Advance System, Aalborg University, 2008
4. B. D. Van Veen and K. M. Buckley, "Beamforming: a versatile approach to spatial filtering," IEEE ASSP Magazine, vol. 5, pp. 4-24, 1988.
5. R. Fallahi, M. Roshandel, Effect of mutual coupling and configuration of concentric circular array antenna on the signal-to-interference performance in CDMA system," Progress in Electromagnetics Research, PIER, vol. 76, 427–447, 2007.
6. Urvinder Singh, Tara Singh Kamal, Concentric Circular Antenna Array Synthesis Using Biogeography Based Optimization," Majlesi Journal of Electrical Engineering, Vol. 6, No. 1, Mar. 2012.
7. V. H. Nascimento, "The normalized LMS algorithm with dependent noise," in Proc. Anais do 19° Simpòsio Brasileiro de Telecomunicações, Fortaleza, Brazil, Mar 2001.
8. D. T. M. Slock, "On the convergence behavior of the LMS and the normalized LMS algorithms," IEEE Trans. on Signal Processing, vol. 41, pp. 2811-2825, 1993.
9. V. H. Nascimento, "Improving the initial convergence of adaptive filters: variable-length LMS algorithms," in Proc. 14th Int. Conf. on Digital Signal Processing, Santorini, Greece, July 2007, pp. 667-670.
10. E. M. Lobato, O. J. Tobias, and R. Seara, "Stochastic modeling of the transform-domain εLMS algorithm for correlated Gaussian data," IEEE Trans. on Signal Processing, vol. 56, pp. 1840-1852, 2008.
11. J. M. Górriz, J. Ramírez, S. Cruces-Alvarez, D. Erdogmus, C. G. Puntonet, and E. W. Lang, "Speech enhancement in discontinuous transmission systems using the constrained-stability least-mean-squares algorithm," Jornal of Acoustical Society of America, vol. 124(6), pp. 3669-3683, Dec. 2008.
12. J. Srar, K. S. Chung, and A. Mansour, "Adaptive array beamforming using a combined LMS-LMS algorithm," IEEE Trans. on Antennas and Propagation, vol. 58, pp. 3545-3557, 2010.
13. M. Dessouky, H. Sharshar, and Y. Albagory, "Efficient sidelobe reduction technique for small-sized concentric circular arrays", Progress in Electromagnetics Research, PIER, vol. 65, 187–200, 2006.